Nonconventional screening of the Coulomb interaction in Fe_xO_y clusters: An *ab initio* study

L. Peters,[1,*] E. Şaşıoğlu,[2,3] S. Rossen,[1,3] C. Friedrich,[3] S. Blügel,[3] and M. I. Katsnelson[1]

[1]*Institute for Molecules and Materials, Radboud University Nijmegen, NL-6525 AJ Nijmegen, The Netherlands*

[2]*Institut für Physik, Martin-Luther-Universität Halle-Wittenberg, D-06099 Halle (Saale) Germany*

[3]*Peter Grünberg Institut and Institute for Advanced Simulation, Forschungszentrum Jülich and JARA, 52425 Jülich, Germany*

(Received 28 November 2016; revised manuscript received 2 March 2017; published 14 April 2017)

From microscopic point-dipole model calculations of the screening of the Coulomb interaction in nonpolar systems by polarizable atoms, it is known that screening strongly depends on dimensionality. For example, in one-dimensional systems, the short-range interaction is screened, while the long-range interaction is antiscreened. This antiscreening is also observed in some zero-dimensional structures, i.e., molecular systems. By means of *ab initio* calculations in conjunction with the random-phase approximation (RPA) within the FLAPW method, we study screening of the Coulomb interaction in Fe_xO_y clusters. For completeness, these results are compared with their bulk counterpart magnetite. It appears that the on-site Coulomb interaction is very well screened both in the clusters and bulk. On the other hand, for the intersite Coulomb interaction, the important observation is made that it is almost constant throughout the clusters, while for the bulk it is almost completely screened. More precisely and interestingly, in the clusters antiscreening is observed by means of *ab initio* calculations.

DOI: 10.1103/PhysRevB.95.155119

I. INTRODUCTION

The huge interest in nanotechnology is fuelling the trend of downscaling devices. Naturally, this will reach the regime of small clusters. However, also from a fundamental point of view, clusters are very interesting. In general, clusters behave completely different from their bulk counterpart. In particular, the removal or addition of just one atom can change the electronic and magnetic properties completely [1–4]. This clearly provides a huge playground for the design of new devices.

For an efficient design, a proper fundamental understanding of the system is essential. This is usually complicated by correlation effects that inhibit an exact solution to the problem. Therefore, in practice, approximate methods have to be considered. In order to find a proper method, knowledge of the correlation effects is crucial. For example, for weakly correlated systems, it is known that density functional theory (DFT) works very well, while for strong local correlations a (generalized) Hubbard model provides a good description. Actually, it is the gradient of the (screened) Coulomb interaction that matters [5]. For a very small gradient, i.e., an almost constant effective Coulomb interaction, clearly a mean-field approach and thus single-particle approach is justified. On the other hand, for a very large gradient, i.e., for only a local effective Coulomb interaction, the Hubbard model becomes adequate.

It is this important information on the effective Coulomb interaction that is provided in this work for the Fe_xO_y clusters. More precisely, Fe_2O_3, Fe_3O_4, and Fe_4O_6 are selected since they are well studied in literature [6–14]. Furthermore, two of them are antiferromagnetic, while the other is ferromagnetic. There exist several methods to calculate the effective Coulomb interaction. For example, in the bulk usually a uniform dielectric theory can be used [15]. Here the system is modeled as a continuum and the (**q**-dependent) dielectric constant is obtained within a mean-field approximation. For example, the Clausius-Mossotti approximation can be used for ionic insulators. Since the dielectric constant depends only on the distance between the charges (and not the crystal structure), this approximation is only good when local field corrections can be neglected. However, it is well known that these local field corrections become important for low dimensional systems. The microscopic point-dipole model can be used to take local field corrections into account [5,15]. This method is based on the assumption that the charge distribution of a polarized system can be considered as a collection of localized point dipoles. This assumption works reasonably for localized charge distributions like in ionic insulators, but becomes inadequate for systems with delocalized charges due to for example covalent bonds. Since it is not clear from the beginning to which regime Fe_xO_y clusters belong, we use *ab initio* theory in conjunction with the random phase approximation (RPA). In this way, also local field corrections are included.

Iron-oxide clusters and nanoparticles have applications in catalysis, magnetic data storage and biomedical treatment due to their unique catalytic, magnetic and biochemical properties [16–18]. Furthermore, iron-oxide interactions are interesting in general for corrosion and biological oxygen transport processes. Thus a detailed understanding of Fe_xO_y clusters could contribute to a better understanding of such processes and new technological applications. Due to this interest there have been a number of experimental and theoretical studies [6–14]. Most theoretical studies are performed with DFT and focus on the geometric structure. From a comparison of the experimental and calculated vibrational spectrum, the structure of some Fe_xO_y clusters is well established [12,13]. Furthermore, some studies address in some detail the electronic and magnetic structure. However, to our knowledge, a detailed consideration of correlation and screening effects does not exist. In our opinion such an understanding is crucial and should form the basis in determining which methods to use for further studies.

The aim of the present work is the *ab initio* determination of the screened Coulomb interaction in Fe_2O_3, Fe_3O_4, and Fe_4O_6 clusters. Employing the random-phase approximation

*L.Peters@science.ru.nl

(RPA) within the full-potential linearized augmented plane wave (FLAPW) method using Wannier functions we show that in these clusters the on-site Coulomb interaction is well screened, while the intersite Coulomb interactions are barely screened or even antiscreened. The important consequence being that the Coulomb interaction is almost constant throughout the clusters. For completeness we compared these results with their bulk counterpart magnetite. Herein only the on-site Coulomb interaction is appreciable, while the intersite Coulomb interactions are almost completely screened. The rest of the paper is organized as follows. The method and computational details are presented in Secs. II and III, respectively. Section IV deals with the results and discussion, and finally in Sec. V, we give the conclusions.

II. METHOD

In this work, we study partially and fully screened Coulomb interaction parameters calculated with the *ab initio* cRPA and RPA methods, respectively. The noninteracting reference system is taken from a preceding DFT calculation.

The effective Coulomb interaction is defined as

$$W(\boldsymbol{r},\boldsymbol{r}',\omega) = \int d\boldsymbol{r}''\epsilon^{-1}(\boldsymbol{r},\boldsymbol{r}'',\omega)v(\boldsymbol{r}'',\boldsymbol{r}'), \tag{1}$$

where $\epsilon(\boldsymbol{r},\boldsymbol{r}'',\omega)$ is the dielectric function and $v(\boldsymbol{r}'',\boldsymbol{r}')$ is the bare Coulomb interaction potential. Since an exact expression for the dielectric function is not accessible, an approximation is required. In the RPA, the dielectric function is approximated by

$$\epsilon(\boldsymbol{r},\boldsymbol{r}',\omega) = \delta(\boldsymbol{r}-\boldsymbol{r}') - \int d\boldsymbol{r}''v(\boldsymbol{r},\boldsymbol{r}'')P(\boldsymbol{r}'',\boldsymbol{r}',\omega), \tag{2}$$

where the polarization function $P(\boldsymbol{r}'',\boldsymbol{r}',\omega)$ is given by

$$\begin{aligned} &P(\boldsymbol{r},\boldsymbol{r}',\omega) \\ &= \sum_{\sigma}\sum_{\boldsymbol{k},m}^{\text{occ}}\sum_{\boldsymbol{k}',m'}^{\text{unocc}} \varphi^{\sigma}_{\boldsymbol{k}m}(\boldsymbol{r})\varphi^{\sigma *}_{\boldsymbol{k}'m'}(\boldsymbol{r})\varphi^{\sigma *}_{\boldsymbol{k}m}(\boldsymbol{r}')\varphi^{\sigma}_{\boldsymbol{k}'m'}(\boldsymbol{r}') \\ &\quad\times\left(\frac{1}{\omega-\Delta^{\sigma}_{\boldsymbol{k}m,\boldsymbol{k}'m'}} - \frac{1}{\omega+\Delta^{\sigma}_{\boldsymbol{k}m,\boldsymbol{k}'m'}}\right). \end{aligned} \tag{3}$$

Here, $\Delta^{\sigma}_{\boldsymbol{k}m,\boldsymbol{k}'m'} = \epsilon^{\sigma}_{\boldsymbol{k}'m'} - \epsilon^{\sigma}_{\boldsymbol{k}m} - i\eta$ with $\epsilon^{\sigma}_{\boldsymbol{k}m}$ the single particle Kohn-Sham eigenvalues obtained from DFT and η a positive infinitesimal. Further, the $\varphi^{\sigma}_{\boldsymbol{k}m}(\boldsymbol{r})$ are the single-particle Kohn-Sham eigenstates with spin σ, wave number $\boldsymbol{k}$, and band index m. The tags "occ" and "unocc" above the summation symbol indicate that the summation is respectively over occupied and unoccupied states only.

Equations (1)–(3) constitute what is called the RPA of the dynamically screened Coulomb interaction. In the *constrained* RPA, the effective Coulomb interaction between a specific type of electrons in the system is considered. For example, in this work, the effective Coulomb interaction between the 3*d* electrons of iron will be investigated. Two types of RPA calculations are performed leading to fully and partially screened (effective U or Hubbard U) Coulomb interaction parameters. In the latter, the screening due to the electrons under consideration is excluded, i.e., in our case the 3*d* electrons of iron. Thus such a cRPA calculation provides the effective interaction that the electrons in the 3*d* Hubbard model would experience; in other words, it yields the corresponding Hubbard U parameter. Obviously, it also gives insight to the importance of these 3*d* electrons in the screening process.

In order to exclude the screening due to certain electrons one separates the polarization function in Eq. (3) as follows:

$$P = P_l + P_r. \tag{4}$$

Here, in our case, P_l includes only transitions between the strongly correlated 3*d* states of iron and P_r is the remainder. Then, the frequency dependent effective Coulomb interaction is given schematically by the matrix equation

$$U(\omega) = [1 - vP_r(\omega)]^{-1}v, \tag{5}$$

where v is the bare Coulomb interaction.

The problem with the separation of Eq. (4) is that it is only well defined for disentangled states. For entangled states different methods have been developed [19–21]. In this work, we use the method described in Ref. [21]. Here we first define the probability to find a strongly correlated electron (3*d* state of iron in our case) in eigenstate $\varphi^{\sigma}_{\boldsymbol{k}m}$ as

$$c^{\sigma}_{\boldsymbol{k}m} = \sum_{i,n}\left|T^{\sigma\boldsymbol{k}}_{i,mn}\right|^2. \tag{6}$$

Here the unitary matrices $T^{\sigma\boldsymbol{k}}_{i,mn}$ are determined from the concept of maximally localized Wannier functions,

$$w^{\sigma}_{in}(\boldsymbol{r}) = \frac{1}{N}\sum_{\boldsymbol{k}} e^{-i\boldsymbol{k}\cdot\boldsymbol{R}_i}\sum_{m} T^{\sigma\boldsymbol{k}}_{i,mn}\varphi^{\sigma}_{\boldsymbol{k}m}(\boldsymbol{r}), \tag{7}$$

where $w^{\sigma}_{in}(\boldsymbol{r})$ is a maximally localized Wannier function located at site i, N is the number of discrete k points in the full Brillouin zone and $\boldsymbol{R}_i$ the position vector of atomic site i. The matrices $T^{\sigma\boldsymbol{k}}_{i,mn}$ are determined by minimizing the spread of the Wannier functions,

$$\Omega = \sum_{i,n,\sigma}\left(\left\langle w^{\sigma}_{in}\middle|r^2\middle|w^{\sigma}_{in}\right\rangle - \left\langle w^{\sigma}_{in}\middle|\boldsymbol{r}\middle|w^{\sigma}_{in}\right\rangle^2\right). \tag{8}$$

Here the sum runs over all Wannier functions. It can be shown that the maximally localized Wannier functions constitute an orthonormal basis and that they resemble atomic orbitals, i.e., they are centered at an atomic site and decay with increasing distance from the site. Further, there is an efficient algorithm to find the $T^{\sigma\boldsymbol{k}}_{i,mn}$ under the condition that the spread is minimized. From Eq. (7), it is clear that a choice has to be made on which bands to include for the construction of the maximally localized Wannier states. In practice (for entangled states), we make sure that enough bands are selected such that all the strongly correlated electron character is contained. Then, in general the number of maximally localized Wannier functions obtained from this space is larger than the dimensions spanned by the strongly correlated electrons. Therefore a selection has to be made. Since the strongly correlated electrons are more localized than the other electrons, the idea is that the subset consisting of the most maximally localized Wannier functions correspond to the strongly correlated electrons.

For entangled states, the probability $c^{\sigma}_{\boldsymbol{k}m} < 1$ in Eq. (6), while for disentangled states $c^{\sigma}_{\boldsymbol{k}m} = 1$. Then, the probability of an electron to be in the 3*d* correlated subspace before and

after a transition $\varphi^{\sigma}_{\boldsymbol{k}m} \rightarrow \varphi^{\sigma}_{\boldsymbol{k}'m'}$ is given by

$$p^{\sigma}_{\boldsymbol{k}m\rightarrow\boldsymbol{k}'m'} = c^{\sigma}_{\boldsymbol{k}m} c^{\sigma}_{\boldsymbol{k}'m'}. \tag{9}$$

Thus for disentangled states $p^{\sigma}_{\boldsymbol{k}m\rightarrow\boldsymbol{k}'m'} = 1$ and for entangled states $p^{\sigma}_{\boldsymbol{k}m\rightarrow\boldsymbol{k}'m'} < 1$. The polarization function P_l now becomes

$$\begin{aligned} &P_l(\boldsymbol{r},\boldsymbol{r}',\omega) \\ &= \sum_{\sigma} \sum_{\boldsymbol{k},m}^{\text{occ}} \sum_{\boldsymbol{k}',m'}^{\text{unocc}} \left(p^{\sigma}_{\boldsymbol{k}m\rightarrow\boldsymbol{k}'m'}\right)^2 \varphi^{\sigma}_{\boldsymbol{k}m}(\boldsymbol{r}) \varphi^{\sigma *}_{\boldsymbol{k}'m'}(\boldsymbol{r}) \varphi^{\sigma *}_{\boldsymbol{k}m}(\boldsymbol{r}') \varphi^{\sigma}_{\boldsymbol{k}'m'}(\boldsymbol{r}') \\ &\times \left(\frac{1}{\omega - \Delta^{\sigma}_{\boldsymbol{k}m,\boldsymbol{k}'m'}} - \frac{1}{\omega + \Delta^{\sigma}_{\boldsymbol{k}m,\boldsymbol{k}'m'}} \right). \end{aligned} \tag{10}$$

By calculating the total polarization from Eq. (3) and P_l from Eq. (10), P_r can be obtained from Eq. (4). For completeness, the effective Coulomb matrix within the selected subspace is computed by

$$\begin{aligned} &U^{\sigma_1,\sigma_2}_{in_1,jn_3,in_2,jn_4}(\omega) \\ &= \iint d\boldsymbol{r} d\boldsymbol{r}' w^{\sigma_1 *}_{in_1}(\boldsymbol{r}) w^{\sigma_2 *}_{jn_3}(\boldsymbol{r}') U(\boldsymbol{r},\boldsymbol{r}',\omega) w^{\sigma_2}_{jn_4}(\boldsymbol{r}') w^{\sigma_1}_{in_2}(\boldsymbol{r}). \end{aligned} \tag{11}$$

In this work, we only consider the static limit ($\omega = 0$). Furthermore, we use Slater parametrization,

$$\begin{aligned} U_i &= \frac{1}{(2l+1)^2} \sum_{m,m'} U^{\sigma_1,\sigma_2}_{im,im',im,im'}(\omega = 0) \quad \text{and} \\ V_{ij} &= \frac{1}{(2l+1)^2} \sum_{m,m'} U^{\sigma_1,\sigma_2}_{im,jm',im,jm'}(\omega = 0). \end{aligned} \tag{12}$$

Here, U_i is the effective on-site Coulomb interaction at site i and V_{ij} the effective intersite Coulomb interaction between sites i and j. Note that although the matrix elements of the Coulomb potential are formally spin-dependent due to the spin dependence of the Wannier functions, we find that this dependence is negligible in practice.

III. COMPUTATIONAL DETAILS

The DFT calculations are performed with the FLEUR code, which is based on a full-potential linearized augmented plane wave (FLAPW) implementation [22]. All calculations are performed with an exchange-correlation functional in the generalized gradient approximation (GGA) as formulated by Perdew, Burke, and Ernzerhof (PBE) [23]. Further, all calculations are without spin orbit coupling.

Since it is a **k**-space code, a supercell approach was employed for the cluster calculations, with a large empty space between clusters that were repeated in a periodic lattice. In our calculations, a large unit cell of at least 12 Å dimensions is used in order to prevent the interaction between clusters of different unit cells. Further, for the cluster calculations the cutoff for the plane waves is 3.6 Bohr^{-1}, $l_{\text{cut}} = 8$ and the Γ point is the only **k**-point considered. The ground-state geometric and magnetic structure of the Fe_2O_3, Fe_3O_4, and Fe_4O_6 clusters is obtained from Refs. [13,14] (see also Fig. 1). More precisely, the geometries are optimized structures obtained from hybrid (B3LYP) functional calculations [24]. The Fe_2O_3 and Fe_4O_6 clusters are antiferromagnetic, while Fe_3O_4 is ferromagnetic.

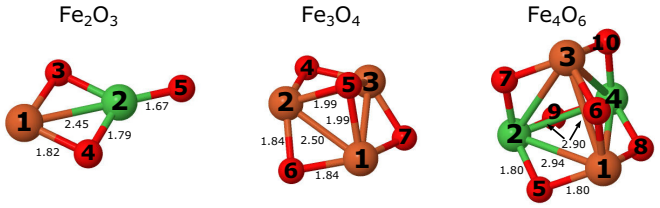

FIG. 1. The geometry of the Fe_2O_3, Fe_3O_4, and Fe_4O_6 clusters. Here the red spheres correspond to the oxygen atoms, while the brown and green spheres correspond to iron atoms with antiparallel local magnetic moments. The distances between some atoms are provided in angstroms.

For magnetite the geometric and magnetic structure is obtained from Refs. [25,26]. Here the structure of magnetite is monoclinic with 56 atoms in the unit cell. The chemical formula is $Fe^{3+}_A[Fe^{2+},Fe^{3+}]_B O_4$ with A referring to tetrahedral sites occupied by Fe^{3+} and B to octahedral sites containing both Fe^{2+} and Fe^{3+}. The magnetic moments of the B sites are antiparallel to those of the A sites. For the **k** mesh a grid of $6 \times 6 \times 2$ equidistant **k** points is used. The cutoff for the plane waves is 4.0 Bohr^{-1} and $l_{\text{cut}} = 8$.

The DFT calculations are used as an input for the SPEX code to perform RPA and cRPA calculations for the screened Coulomb interaction [27]. The SPEX code uses the WANNIER90 library to construct the maximally localized Wannier functions [28,29]. For this construction we used six states per iron atom, i.e., five $3d$ states and one $4s$ state.

IV. RESULTS AND DISCUSSION

In Fig. 1, the geometry and magnetic structure of the Fe_2O_3, Fe_3O_4, and Fe_4O_6 clusters is depicted. The red spheres correspond to the oxygen atoms, while the brown and green spheres correspond to iron atoms with antiparallel local magnetic moments. The distances between some of the atoms are given in Å. Further, Fe_2O_3 and Fe_4O_6 are antiferromagnetic, while Fe_3O_4 is ferromagnetic. From Fe_4O_6, it can be observed that the direction of the local magnetic moment has a small influence on the bonding, i.e., the distance between two iron atoms with parallel and antiparallel moments is 2.90 and 2.94 Å.

In the following, we will discuss the matrix elements of the fully screened Coulomb interaction (RPA) as well as the partially screened effective Coulomb interaction (cRPA) for Fe_xO_y clusters. The latter is important in dealing with correlation effects in clusters as well as it provides information on the contribution of the Fe($3d$) $\rightarrow$ Fe($3d$) screening channel to the total screening process. In Table I, the bare and fully screened on-site and intersite average Coulomb interaction parameters for Fe-$3d$ and O-$2p$ orbitals are presented for all three Fe_xO_y clusters. Note that due to symmetry for each cluster some iron and oxygen atoms are equivalent. For the smallest Fe_2O_3 cluster oxygen atoms 3 and 4 are equivalent, while for the Fe_3O_4 cluster all iron atoms and oxygen atoms 4, 6, and 7 are equivalent. In the case of the largest Fe_4O_6 cluster, iron atoms 1, 3 and 2, 4 are equivalent, while for

TABLE I. The bare (unscreened) and fully screened (RPA) average Coulomb interaction parameters for the Fe-3*d* and O-2*p* orbitals of the Fe_xO_y clusters obtained from *ab initio* calculations. Here U_1 corresponds to the on-site Coulomb interaction of atom 1 and $V_{1,2}$ to the intersite Coulomb interaction between atoms 1 and 2 (see Fig. 1). The second column indicates between what type of atoms this refers and the third column corresponds to the distance (in Å) between them. Note that due to symmetry oxygen atoms 3 and 4 are equivalent for the Fe_2O_3 cluster. While in Fe_3O_4 cluster all iron atoms and oxygen atoms 4, 6, and 7 are equivalent. In the case of Fe_4O_6 cluster, iron atoms 1, 3 and 2, 4 are equivalent, while for oxygen atoms 5, 7, 8, 10 and 6, 9 are equivalent. In bold face, the intersite Coulomb interactions at which antiscreening occurs are presented.

		Fe_2O_3		
U/V	Atom	Distance (Å)	Bare (eV)	RPA (eV)
U_1	Fe	0	21.7	7.7
U_2	Fe	0	22.2	7.8
U_3	O	0	17.8	8.2
U_5	O	0	17.7	7.9
$V_{2,5}$	Fe-O	1.67	8.6	6.7
$V_{2,3}$	Fe-O	1.79	8.0	6.5
$V_{1,3}$	Fe-O	1.82	7.8	6.4
$V_{1,2}$	Fe-Fe	2.45	5.9	**6.5**
$V_{3,4}$	O-O	2.66	5.6	**6.0**
$V_{3,5}$	O-O	3.16	4.8	**6.0**
$V_{1,5}$	Fe-O	4.11	3.9	**6.0**
		Fe_3O_4		
U/V	Atom	Distance (Å)	Bare (eV)	RPA (eV)
U_1	Fe	0	22.2	7.4
U_4	O	0	17.8	7.8
U_5	O	0	17.9	8.1
$V_{1,6}$	Fe-O	1.84	7.8	5.8
$V_{1,5}$	Fe-O	1.99	7.2	5.7
$V_{1,2}$	Fe-Fe	2.50	5.8	5.8
$V_{4,5}$	O-O	2.73	5.4	5.3
$V_{4,6}$	O-O	3.40	4.5	**5.1**
$V_{1,4}$	Fe-O	3.45	4.4	**5.3**
		Fe_4O_6		
U/V	Atom	Distance (Å)	Bare (eV)	RPA (eV)
U_1	Fe	0	22.3	5.9
U_3	Fe	0	22.3	5.9
U_5	O	0	18.1	6.8
U_6	O	0	18.0	7.0
$V_{1,5}$	Fe-O	1.80	8.0	5.1
$V_{1,6}$	Fe-O	1.83	7.8	5.0
$V_{1,3}$	Fe-Fe	2.90	5.1	**5.3**
$V_{5,7}$	O-O	2.92	5.1	4.8
$V_{1,2}$	Fe-Fe	2.94	5.0	**5.2**
$V_{5,6}$	O-O	3.00	5.0	4.8
$V_{5,9}$	O-O	3.00	5.0	4.8
$V_{1,7}$	Fe-O	3.43	4.4	**5.0**
$V_{1,9}$	Fe-O	3.54	4.3	**4.9**
$V_{5,10}$	O-O	4.13	3.8	**4.7**
$V_{6,9}$	O-O	4.34	3.7	**4.7**

oxygen atoms 5, 7, 8, 10 and 6, 9 are equivalent. Thus only symmetry unequivalent interactions are presented. As seen for all three clusters the on-site Coulomb interactions are very well screened. On the other hand the intersite Coulomb interaction is much less screened and is more or less constant as function of intersite distance.

Considering the smallest Fe_2O_3 cluster, starting from an intersite distance of 2.45 Å antiscreening is observed (bold face numbers in Table I), i.e., the fully screened interaction is larger than the bare interaction. For example, for the intersite Coulomb interaction between the two iron atoms, the antiscreening contribution is 0.6 eV and between iron atom 1 and oxygen atom 5 it is even 2.1 eV. Also in the other two clusters, Fe_3O_4 and Fe_4O_6, antiscreening is observed. Although, as seen in Table I for Fe_3O_4 antiscreening starts to occur at a larger intersite distance. More precisely, between two iron atoms the bare and fully screened Coulomb interactions are equal and therefore there is strictly speaking no antiscreening. On the other hand between two oxygen atoms, and iron and oxygen antiscreening occurs at respectively 3.40 and 3.35 Å. Here the antiscreening contribution is 0.6 eV for the former and 0.9 eV for the latter. For Fe_4O_6, the antiscreening is a bit more complex. It occurs between two iron atoms at intersite distances of 2.90 and 2.94 Å, while it is absent between two oxygen atoms until an intersite distance of 4.13 Å. Between iron and oxygen antiscreening starts at an intersite distance of 3.43 Å.

The total screening calculated via *ab initio* can be decomposed into different screening channels. For the present systems the main contribution to the screening process stems from the O(2*p*) and Fe(3*d*) states present around the chemical potential via O(2*p*) $\rightarrow$ O(2*p*), O(2*p*) $\rightarrow$ Fe(3*d*), and Fe(3*d*) $\rightarrow$ Fe(3*d*) transitions. As the O(2*p*) states are fully occupied their contribution to the total polarization function is small [see Eq. (3)]. In order to investigate the influence of the Fe(3*d*) $\rightarrow$ Fe(3*d*) transitions for the Fe(3*d*) orbitals, we present in Table II the partially screened Coulomb interaction parameters for the Fe(3*d*) orbitals by excluding Fe(3*d*) $\rightarrow$ Fe(3*d*) transitions. It can be observed that for all three clusters for the on-site Coulomb interaction this contribution is very small, about 1 eV, compared to that of the Fe(3*d*) $\rightarrow$ O(2*p*) screening channel of more than 13 eV. On the hand for the intersite iron-iron

TABLE II. The partially screened (cRPA) average Coulomb interaction parameters for the Fe(3*d*) orbitals of the Fe_xO_y cluster obtained from *ab initio* calculations. Here, U_1 corresponds to the on-site Coulomb interaction of atom 1 and $V_{1,2}$ to the intersite Coulomb interaction between atoms 1 and 2 (see Fig. 1 to which atoms these numbers refer). For comparison, the bare Coulomb interaction parameters are presented in parenthesis.

cRPA (eV)	Atom	Fe_2O_3	Fe_3O_4	Fe_4O_6
U_1	Fe	8.7 (21.7)	8.6 (22.2)	6.9 (22.3)
U_2	Fe	8.9 (22.2)	8.6 (22.2)	6.9 (22.3)
U_3	Fe		8.6 (22.2)	6.9 (22.3)
U_4	Fe			6.9 (22.3)
$V_{1,2}$	Fe	6.3 (5.9)	5.5 (5.8)	5.2 (5.0)
$V_{1,3}$	Fe		5.5 (5.8)	5.4 (5.1)
$V_{2,3}$	Fe		5.5 (5.8)	5.2 (5.1)
$V_{1,4}$	Fe			5.2 (5.0)
$V_{2,4}$	Fe			5.4 (5.1)
$V_{3,4}$	Fe			5.2 (5.0)

Coulomb interaction the Fe($3d$) → Fe($3d$) channel contributes significantly, 0.2 eV, to the total antiscreening effect of 0.6 eV in the case of smallest cluster Fe_2O_3. For the Fe_3O_4 cluster, there is no antiscreening contribution from the Fe($3d$) → O($2p$) channel, i.e., it reduces the bare interaction by about 0.3 eV, while the Fe($3d$) → Fe($3d$) channel has an antiscreening contribution of 0.3 eV. For the largest cluster Fe_4O_6, it appears from Table II that there is no antiscreening contribution from the Fe($3d$) → Fe($3d$) channel. Instead there is a very small screening contribution of 0.1 eV between two iron atoms with parallel magnetic moments and no contribution between two iron atoms with antiparallel moments. Finally, as the cluster size increases the effective on-site Coulomb interaction parameters for Fe($3d$) electrons decreases from 8.7 to 6.9 eV as expected.

Previous studies have shown that antiscreening strongly manifest itself in low-dimensional semiconductors and insulators [5,30]. Using a point-dipole interaction model van den Brink and Sawatsky calculated the screened intersite Coulomb interaction for finite size systems like molecules (benzene, naphtaline, C_{60}, etc.) and one-dimensional atomic chains [5]. The authors found that, in contrast to three-dimensional bulk semiconductors, in low-dimensional systems the local field effects play a very important role in screening of the Coulomb interaction. It turns out that the Coulomb interaction is strongly r-dependent, i.e., at short distances, it is strongly screened, at intermediate distances it is antiscreened, and at large distances it is unscreened. The occurrence of antiscreening in low-dimensional systems was attributed to the sign change of the induced polarization around the test charge with distance. In three-dimensional insulators and semiconductors, the induced polarization is negative over all space, while in low-dimensional systems, it can change sign with distance resulting in an antiscreening. The critical distance r_c, where the transition from screening to antiscreening takes place, depends very much on the dimensionality and polarization of the system. For instance, in zero-dimensional molecules (benzene, naphthalene) r_c is rather small, 3–4 Å [5], while in quasi-one-dimensional single-wall carbon nanotubes, it is around 20 Å [30]. For the Fe_xO_y clusters considered in the present work, the critical distance r_c can be even shorter than the zero dimensional systems studied in literature. Here the critical distance is estimated by the first intersite distance at which antiscreening occurs. Then, for Fe_2O_3, Fe_3O_4, and Fe_4O_6 the critical distance is respectively 2.45, 3.40, and 2.90 Å. Note that even in three-dimensional bulk materials the nonlocal antiscreening takes place within the subspace of the correlated electrons as recently shown by Nomura *et al.*, for the case of $SrVO_3$ [31].

It is interesting to compare these cluster results with their bulk counterpart magnetite. In Table III, the calculated results are shown for magnetite. Here the first column shows on or between which sublattices the interaction is considered and the second column contains the distance between these sublattices (a zero indicates an on-site interaction). For the sublattices, the same nomenclature is adopted as in Ref. [25]. From Table III, it can be observed that the intersite Coulomb interaction is almost completely screened, which is in strong contrast with the zero-dimensional cluster results. The on-site Coulomb interaction is also more screened than for the clusters. Furthermore, the cRPA calculations reveal that the effect of the screening due to the iron $3d$ states in magnetite is quite a bit larger than for the clusters.

TABLE III. The bare, partially screened (cRPA) and fully screened (RPA) average Coulomb interaction parameters for the Fe-$3d$ orbitals of magnetite obtained from *ab initio* calculations. Here the first column shows on or between which sublattice the interaction is considered and the second column contains the distance between these sublattices (a zero referring to an on-site interaction). For the sublattices the same nomenclature is adopted as in Ref. [25].

	r(Å)	Bare (eV)	cRPA (eV)	RPA (eV)
A1	0	22.9	4.3	1.53
A2	0	22.9	4.3	1.51
B1a	0	22.9	4.8	0.75
B1b	0	22.9	4.8	0.77
B2a	0	22.9	4.7	0.82
B3	0	22.9	4.6	0.81
A1-A2	6.93	2.4	0.01	0.01
B1a-B2a	5.10	3.0	0.09	0.02
B1a-B1b	2.97	4.9	0.35	0.02
B1b-B3	2.86	5.1	0.37	0.04

Finally, we would like to comment on the strength of the electronic correlations in three-dimensional magnetite Fe_3O_4 and zero-dimensional Fe_xO_y clusters. The short-range nature of the Coulomb interaction with large gradient in magnetite makes it a correlated material and thus electronic structure methods which go beyond the standard DFT are necessary for an accurate description of the electronic structure of magnetite. For instance, the experimentally observed charge order in magnetite cannot be captured in DFT. From Ref. [25], it is known that an additional treatment of the on-site correlations between the Fe $3d$ electrons is needed. It was found that the DFT+U approach, a static mean-field treatment of on-site correlations, gives a charge ordering in agreement with experiment. On the other hand, due to the almost constant Coulomb interaction in zero-dimensional Fe_xO_y clusters, DFT calculations employing standard functionals can be expected to capture the essential physics. For example, from a comparison of the experimental vibrational spectrum with the theoretical spectra of different isomers and magnetic structures, the geometric and magnetic structure are obtained in good agreement with the experiment [12,14].

V. CONCLUSION

We have performed RPA (and cRPA) calculations to investigate the screening of the Coulomb interaction in the Fe_2O_3, Fe_3O_4, and Fe_4O_6 clusters and their bulk counterpart magnetite. It has been demonstrated that both in the clusters and bulk the on-site Coulomb interaction is very well screened. Here the main screening contribution stems from the Fe($3d$) → O($2p$) channel. On the other hand the intersite Coulomb interaction is barely screened or even antiscreened in the clusters, while in the bulk it is almost completely screened. In Fe_2O_3 and Fe_3O_4, the antiscreening starts at a certain intersite distance, 2.45 and 3.40 Å respectively. For Fe_4O_6 the antiscreening nature is a bit more complex. It first occurs at a distance of

2.90 Å, then both screening and antiscreening can be observed until a distance of 3.43 Å from which on it is of antiscreening nature only. The important consequence is that in the clusters the Coulomb interaction is almost constant, while in the bulk, it has a large gradient. Therefore a proper treatment of correlations are expected to be more important for the bulk than the clusters.

ACKNOWLEDGMENTS

The Nederlandse Organisatie voor Wetenschappelijk Onderzoek (NWO) and SURFsara are acknowledged for the usage of the LISA supercomputer and their support. L.P. and M.I.K. acknowledges a support by European Research Council (ERC) Grant No. 338957.

[1] F. Liu, S. N. Khanna, and P. Jena, Phys. Rev. B **43**, 8179 (1991).

[2] C. N. van Dijk, T. Rasing, A. Kirilyuk, J. Bowlan, A. Liang, and W. A. de Heer, J. Appl. Phys. **107**, 09B526 (2010).

[3] L. Peters, I. Di Marco, M. S. Litsarev, A. Delin, M. I. Katsnelson, A. Kirilyuk, B. Johansson, B. Sanyal, and O. Eriksson, Phys. Rev. B **92**, 035143 (2015).

[4] L. Peters, S. Ghosh, B. Sanyal, C. van Dijk, J. Bowlan, W. de Heer, A. Delin, I. Di Marco, O. Eriksson, M. I. Katsnelson, B. Johansson, and A. Kirilyuk, Sci. Rep. **6**, 19676 (2016).

[5] J. van den Brink, and G. A. Sawatzky, Europhys. Lett. **50**, 447 (2000).

[6] N. M. Reilly, J. U. Reveles, G. E. Johnson, S. N. Khanna, and A. W. Castleman, J. Phys. Chem. A **111**, 4158 (2007).

[7] L. S. Wang, H. Wu, and S. R. Desai, Phys. Rev. Lett. **76**, 4853 (1996).

[8] D. Schröder, P. Jackson, and H. Schwarz, Eur. J. Inorg. Chem. **2000**, 1171 (2000).

[9] A. Erlebach, H. D. Kurland, J. Grabow, F. A. Müller, and M. Sierka, Nanoscale **7**, 2960 (2015).

[10] B. V. Reddy, F. Rasouli, M. R. Hajaligol, and S. N. Khanna, Fuel **83**, 1537 (2004).

[11] B. V. Reddy and S. N. Khanna, Phys. Rev. Lett. **93**, 068301 (2004).

[12] A. Kirilyuk, A. Fielicke, K. Demyk, G. von Helden, G. Meijer, and T. Rasing, Phys. Rev. B **82**, 020405 (2010).

[13] A. Erlebach, C. Hühn, R. Jana, and M. Sierka, Phys. Chem. Chem. Phys. **16**, 26421 (2014).

[14] R. Logemann, G. A. de Wijs, M. I. Katsnelson, and A. Kirilyuk, Phys. Rev. B **92**, 144427 (2015).

[15] T. C. Choy, *Effective Medium Theory Principle and Applications* (Oxford University Press, Oxford, 2016).

[16] R. M. Cornell and U. Schwertmann, *The Iron Oxides: Structure, Properties, Reactions, Occurrences and Uses* (Wiley-VCH, Weinheim, 2003).

[17] S. Laurent, D. Forge, M. Port, A. Roch, C. Robic, L. V. Elst, and R. N. Muller, Chem. Rev. **108**, 2064 (2008).

[18] A. Schätz, O. Reiser, and W. J. Stark, Chem. Eur. J. **16**, 8950 (2010).

[19] F. Aryasetiawan, K. Karlsson, O. Jepsen, and U. Schönberger, Phys. Rev. B **74**, 125106 (2006).

[20] T. Miyake, F. Aryasetiawan, and M. Imada, Phys. Rev. B **80**, 155134 (2009).

[21] E. Şaşıoğlu, C. Friedrich, and S. Blügel, Phys. Rev. B **83**, 121101(R) (2011).

[22] www.flapw.de.

[23] J. P. Perdew, K. Burke, and M. Ernzerhof, Phys. Rev. Lett. **77**, 3865-3868 (1996).

[24] P. J. Stephens, J. F. Devlin, C. F. Chabalowski, and M. J. Frisch, J. Phys. Chem. **98**, 11623 (1994).

[25] H. T. Jeng, G. Y. Guo, and D. J. Huang, Phys. Rev. Lett. **93**, 156403 (2004).

[26] J. P. Wright, J. P. Attfield, and P. G. Radaelli, Phys. Rev. Lett. **87**, 266401 (2001).

[27] C. Friedrich, S. Blügel, and A. Schindlmayr, Phys. Rev. B **81**, 125102 (2010).

[28] A. A. Mostofi, J. R. Yates, Y.- S Lee, I. Souza, D. Vanderbilt, and N. Marzari, Comput. Phys. Commun. **178**, 685 (2008).

[29] F. Freimuth, Y. Mokrousov, D. Wortmann, S. Heinze, and S. Blügel, Phys. Rev. B **78**, 035120 (2008).

[30] J. Deslippe, M. Dipoppa, D. Prendergast, M. V. O. Moutinho, R. B. Capaz, and S. G. Louie, Nano Lett. **9**, 1330 (2009).

[31] Y. Nomura, M. Kaltak, K. Nakamura, C. Taranto, S. Sakai, A. Toschi, R. Arita, K. Held, G. Kresse, and M. Imada, Phys. Rev. B **86**, 085117 (2012).